Tuning Gold Nanorod Synthesis Through Pre-reduction with Salicylic Acid

Leonardo Scarabelli[1], Marek Grzelczak[1,2], Luis M. Liz-Marzán[1,2,*]

[1] *CIC biomaGUNE, Paseo de Miramón 182, 20009 Donostia - San Sebastián, Spain*

[2] *Ikerbasque, Basque Foundation for Science, 48011 Bilbao, Spain*

* Corresponding author: llizmarzan@cicbiomagune.es

ABSTRACT

Successful synthesis of gold nanorods requires subtle combination of additives and reducing species. The latter are of major importance, as the reducing power determines the rate of metallic gold formation, which often defines the final shape and anisotropy. Ascorbic acid is a common reducing agent in the synthesis of gold nanorods, but its relatively strong reducing power limits the tunability of the final shape and optical response. We propose here a bimodal reducing agent system comprising a combination of salicylic and ascorbic acid. While salicylic acid pre-reduces Au(III) to Au(I) in the growth solution, ascorbic acid participates in the autocatalytic reduction of Au(I) to Au(0), selectively occurring on the metallic surface. This combination provides a fine control over gold reduction at any stage of nanorods formation, which in turn leads to improved monodispersity, better reduction yield and morphology control.

Keywords: gold nanorods, salicylic acid, ascorbic acid, growth mechanism

Introduction

The influence of different types of additives on the yield, monodispersity and reproducibility of gold nanorod (NR) synthesis has recently acquired major relevance. The nature of these additives (co-factors) ranges from inorganic anions or cations to both aromatic and aliphatic molecules. A recent example is the study by DuChene et al.,[1] who compared the effects of different halide anions (Cl^-, Br^- and I^-), proposing a growth model based on facet-selective adsorption on the different crystallographic facets present in citrate capped gold seeds, to explain anisotropic growth into different shapes. Similar arguments have been used to explain reshaping upon silver coating, which were in agreement with density functional theory (DFT) calculations of surface energies.[2] Silver ions have also been extensively shown to improve the control and tunability on the aspect ratio (AR) of NRs.[3] Even after a decade, the specific role of silver is however still under debate within the scientific community.[4,5] The two mechanisms that have been most commonly accepted in the literature are the formation of a AgBr (or Ag^+CTABr^- complex)[6] layer and the deposition of Ag^0 atoms by underpotential deposition (UPD)[7] on the surface of the growing particles. On the other hand, Murray and co-workers have recently proposed sodium oleate as an additive to hexadecyltrimethylammonium bromide (CTAB) and to a binary surfactant mixture.[8] This allowed them to access unusual experimental conditions (i.e. lower seed concentration and higher Ag/Au ratios), thereby leading to NRs with larger dimensions, wide AR tunability and better monodispersity. The same group showed[9] that aromatic additives such as salicylic acid (and similar molecules) and salicylate salts can interact through hydrophobic interactions with CTAB, intercalating in the bilayer and allowing a better degree of control on the shape and size of the NRs. Interestingly, salicylic acid has been long known as an effective reducing agent for the preparation of gold nanoparticles.[10] This was also

exploited by Malikova et al.[11] for the preparation of nanoprisms in aqueous media at high temperature, as well as by Luo,[12] who achieved an increase in the yield of nanoplates and their size by adding a certain amount of poly(diallyldimethylammonium chloride) to the growth solution.

Despite all these efforts to improve the quality and variability in the synthesis of gold NRs, the detailed mechanism through which NRs evolve from isotropic seeds has not yet been fully understood. In this context, the mechanistic study of the influence of additives can supply new ideas in this field, and shed light on the points that are still unresolved. Regarding the silver assisted synthesis of gold NRs, different groups agree in identifying two separate stages during the growth process, which are reflected in changes of the optical spectra: a fast redshift of the longitudinal band during the first minutes of growth, followed by a slow blueshift.[13–16] The former is directly related to the increase of anisotropy that takes place at early stages of growth, whereas the latter is attributed to either isotropic growth[13] or reshaping of the NRs tips,[14,15] as recently supported by different computational[15,17,18] and experimental work, including transmission electron microscopy (TEM)[14] and cryo-TEM[15] studies. It is also important to realize that another open question concerns the yield in terms of gold ions that are effectively reduced. Murphy et al. performed elemental analysis, showing that in the case of silver assisted gold NR growth, only 15% of the gold precursor is effectively reduced, while in the silver-free synthesis the process is quantitative.[19,20]

In this context, we have undertaken the study of the roles of 5-bromosalicylic acid (5-BrSA), as both co-factor and reducing agent for the Au(III)-to-Au(I) reduction step. Our results demonstrate that the use of 5-BrSA opens up the possibility of exploiting this double-reducing-agent-system to tune the AR of the formed particles, while significantly improving the yield of

gold reduction. This may lead to new insights in the mechanistic aspects of the synthesis of anisotropic gold nanoparticles, while offering new strategies toward the control of their shape and dimensions. The reducing power of salicylic acids can also be exploited to perform an overgrowth reaction in a widely controllable way, with different compositions of the overgrowth solutions. In this way we demonstrate that Ag^+ ions help maintaining the NRs anisotropy even after multiple overgrowth steps, thus avoiding a complete loss of anisotropy as registered in the case of silver-free overgrowth conditions.

Results and Discussion

The starting point of our discussion is an observation from ref. 9, regarding the reducing ability of salicylic acid: "The CTAB-additive-$HAuCl_4$ solution becomes colorless after being mixed for about 30 min without ascorbic acid. However, no gold NRs are obtained unless […] ascorbic acid solution is added to the growth solution". Since the loss of color of the "CTAB-additive-$HAuCl_4$ solution" very likely indicates the reduction of Au(III) into Au(I) by "the additive", we studied the kinetics of Au(III) reduction by 5-BrSA in aqueous/CTAB solution, by monitoring the changes in the UV-visible absorbance band of the Au(III)-CTAB complex (λ_{MAX} = 396 nm, inset Figure 1A). It can be observed that the reduction proceeds rather slowly at room temperature (Figure 1), thus providing us with the possibility to precisely select the amount of gold precursor that has been reduced into Au(I) prior to ascorbic acid (AA) addition and to study how this affects the final NR product. The precise nature of the final reduction step is still under debate. Whereas some groups proposed a disproportionation mechanism[21] (catalyzed by the Au(0) surface), where three Au(I) ions would disproportionate into two Au(0) atoms and one

Au(III) ion, other studies suggest that in the presence of CTAB, Au(III) and Au(0) would favorably undergo a comproportionation reaction[22,23]. In the former process, the reducing agent would act as a scavenger to reduce newly formed Au(III) into Au(I), and for this reason we believe that it is unlikely to be the main process in our system, since 5-BrSA should be able to carry out the same scavenging process. As mentioned above, experimental evidence shows that 5-BrSA is unable to initiate NR growth. The synthetic process can thus be described through the following sequence (see also Scheme S1, Supporting Information): i) 5-BrSA is used to partially reduce Au(III) into Au(I) in a pre-reduction step; ii) AA is added to complete the reduction of Au(III); iii) pre-synthesized Au(0) spherical seeds are added, which catalyze the final reduction of Au(I) into Au(0), thereby initiating nanorod growth. It is important to point out that in all the presented experiments other parameters (such as Ag^+ concentration or pH) were kept constant.

As can be seen in Figure 1, the pre-reduction time (monitored following the drop in absorbance at 396 nm, green dots in Figure 1A) strongly affects the final AR of the NRs (Figure 1B). The longitudinal LSPR can be tuned between 850 and 650 nm for shorter and longer pre-reduction times, respectively, corresponding to AR values of 3.9 and 2.4, respectively (Figure 1C). Note that monodispersity is hardly affected, as confirmed by the AR histograms (Figures S1 and S2, Supporting Information). The pre-reduction time also affects significantly the reduction yield, i.e. the final amount of metallic gold. In order to quantify this parameter, we monitored the absorbance at 400 nm, considering that at this wavelength only interband transitions are relevant and therefore the absorbance is independent of particle size. Assuming an absorbance of 1.2 at 400 nm as the corresponding value for 100% reduction[23] using a cuvette with 1cm optical length (quantitative experimental evidence behind this assumption is provided in the Supporting Information, Figure S4), the percentage of unreacted Au(I) may be as high as 75% for the NRs

with the highest AR (shortest pre-reduction time). Assuming the absence of secondary nucleation, i.e. that an 'x' amount of seeds leads to a corresponding 'x' amount of NRs, these data match with the average volume for a single NR, as calculated from TEM analysis (Figure S3, Supporting Information), meaning that smaller rods are formed from the same number of seeds when the pre-reduction time is shorter.

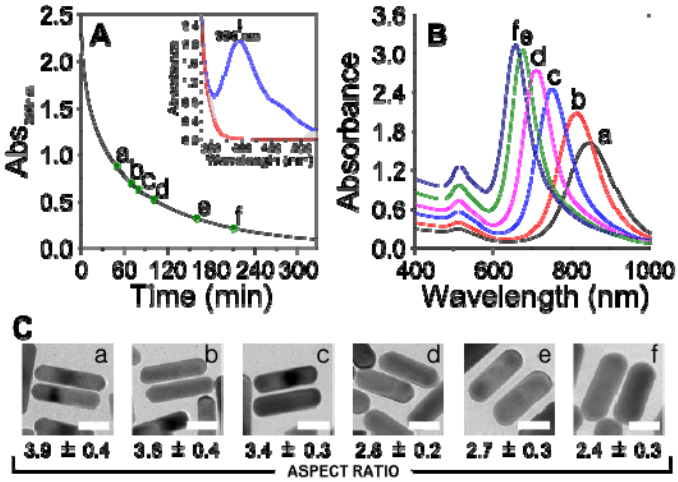

Figure 1. The extent of pre-reduction by 5-BrSA affects both the AR and the amount of reduced gold. **A:** Kinetic study of the pre-reduction step (inset: full UV-vis spectra). **B:** UV-vis-NIR spectra of the various NR colloids obtained by changing the pre-reduction time. Abs_{396nm}: 0.88 (a); 0.71 (b); 0.64 (c); 0.53 (d); 0.33 (e); 0.22 (f) (UV-vis spectra were multiplied by the corresponding dilution factor). **C:** Representative TEM images of NRs obtained with different pre-reduction times (the labels correspond to those on the spectra in B). Scale bars: 20 nm (Further details are provided in the Supporting Information).

To better understand the effect of pre-reduction time, we spectroscopically monitored NRs growth. For this purpose we choose three different pre-reduction times corresponding to Abs_{396nm}

= 0.75, 0.45 and 0.20. As shown in Figure 2, regardless of pre-reduction time, we observed that the longitudinal LSPR initially redshifts, but then progressively blueshifts back, and this blueshift occurs to a larger extent when the pre-reduction time was longer. Additionally, the reduction is completed before the blueshift stops (compare upper and lower plots in Figure 2A), which clearly demonstrates that the blueshift is related to both reduction and reshaping. To correlate the optical behavior with size and shape evolution we arrested the growth of the nanoparticles by addition of excess dodecanethiol,[13,24] at three different stages: (*a*) at the time of maximum LSPR wavelength; (*b*) when gold salt has been totally consumed; (*c*) four hours after seed addition. In all cases, we observed that at stage *a* the nanocrystals have already acquired a well-defined rod-like shape, with similar values of length, width and volume (Figure S5, Supporting Information). At stage *b*, the average NR volume was found to increase further for longer pre-reduction times, as more gold atoms were reduced. We observed that the highest aspect ratio is obtained for the rods prepared with the shortest pre-reduction time, i.e. with the largest amount of unreduced gold salt remaining in the growth solution. In agreement with the UV-vis analysis, the volume of the particles did not increase further at stage *c*. As the amount of added ascorbic acid was constant for all reactions, gold reduction was faster for longer pre-reduction times, when less Au(III) was present in solution and more AA was involved in NR growth (Figure 2A). Incidentally, reshaping of the nanoparticles can be noticed during the whole growth process, resulting in a progressive blueshift for all three samples, which is more pronounced for longer pre-reduction times. In addition, detailed shape inspection of the particles at stage *a* clearly showed that the nanorods obtained at longer pre-reduction times display a certain dumbbell-like morphology. Therefore, we postulate that the deviation from the ideal rod-

like morphology is somehow correlated to the growth rate, and that this affects the final aspect ratio of the NRs.

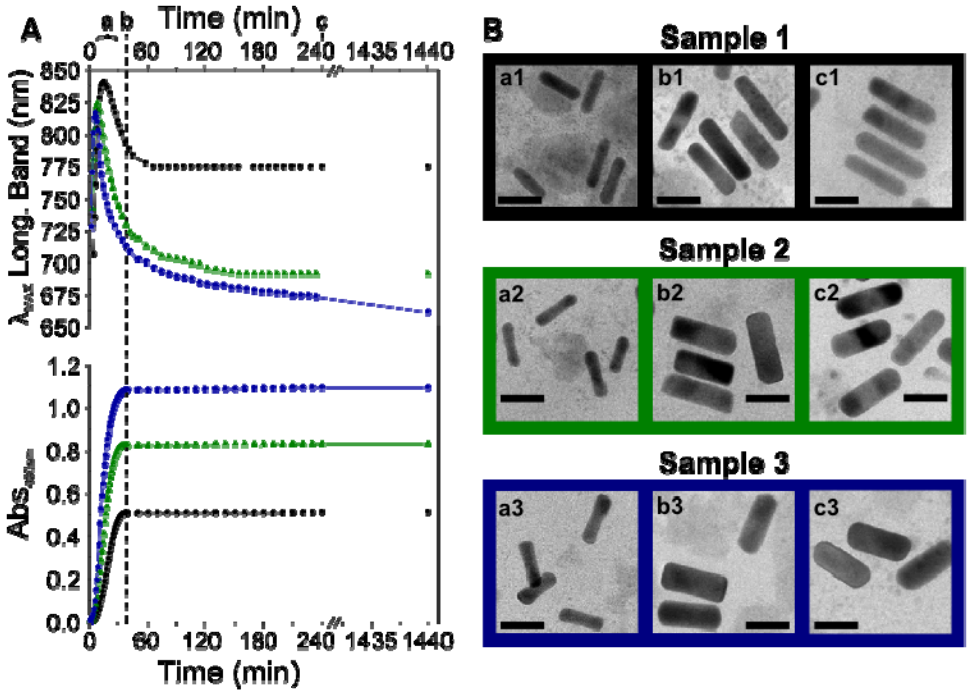

Figure 2. A: Time traces of the longitudinal LSPR and the absorbance at 400 nm during the growth of Au NRs after different pre-reduction times. Pre-reduction was stopped at Abs_{396nm} = 0.75 (sample 1, black), 0.45 (sample 2, green) and 0.20 (sample 3, blue). The vertical dashed line indicates the moment at which no further gold reduction was observed, whereas a, b and c correspond to the times at which the growth was arrested by thiol addition. **B:** TEM images for the three samples collected after addition of dodecanethiol. The labels indicate the different times at which growth was arrested (a, b, c) for each sample (1, 2, 3). Scale bars: 30 nm.

To further confirm the above conclusion, we devised a new set of experiments in which the concentration of ascorbic acid was adjusted as a function of pre-reduction time, so that the total amount of electrons used in the reduction was fixed (For more details see the caption of Figure S6, Supporting Information). For four different experiments, we found that both the aspect ratio and the kinetics of reduction and growth remain unchanged, i.e. the kinetic evolution of the absorbance at 400 nm and the longitudinal LSPR follow the same trend (Figure S6, Supporting Information). These results point again toward the importance of the growth rate to tune the final AR: by modifying the amount of AA to compensate the different extent of pre-reduction, identical initial conditions for NR growth were reproduced, and thus the same final product was obtained.

One important point needs be clarified yet: one may claim that the tunability shown in Figure 1 can be only apparent, and in particular just correlated to the different yield in Au(0). Thus, to complete gold reduction and push all the samples to the same total amount of gold reduced, we added an additional amount of AA. Assuming again that absorbance 1.2 at 400 nm corresponds to complete gold reduction (0.5 mM), the exact amount of AA can be calculated to complete gold reduction (assuming a quantitative two electrons reaction). We exemplify this process with three different samples (prepared with different pre-reduction times) containing known amounts of unreacted Au(I) and added the corresponding amount of AA without any prior washing. All three samples were indeed found to reach the same expected final absorbance at 400 nm of 1.2 (Figure 3A). We also confirmed that, even when a significant excess of AA (up to 35%) was added, no further reduction was achieved (Abs_{400} did not increase). Additional confirmation was provided by calculation of the average NR volumes calculated from the TEM dimensions (Figure 3B). As expected, the volume increase was proportional in all cases to the amount of initially

unreacted Au(I), and the final volume was equal for all samples, even though the AR was different (Figure 3C). This indeed demonstrates that the tunability of the AR shown in Figure 1 was not an artifact created by the different yields in Au(0), and supports the assumption that the number of grown particles is related to the amount of seeds, regardless of other synthetic conditions. It is important to underline here that this possibility cannot be obtained just by changing the AA concentration: in fact, in the standard synthesis the window of AA concentrations that lead to high yield and NR monodispersity is very narrow; moreover the final absorbance at 400 nm cannot be tuned in such a wide range.[25,26] In this respect, the two-reducing-agents system offers the chance to tune the final AR and Au(0) concentration by simply monitoring and selecting the pre-reduction step, with the result of a significant improvement in the reproducibility of the synthetic protocol.

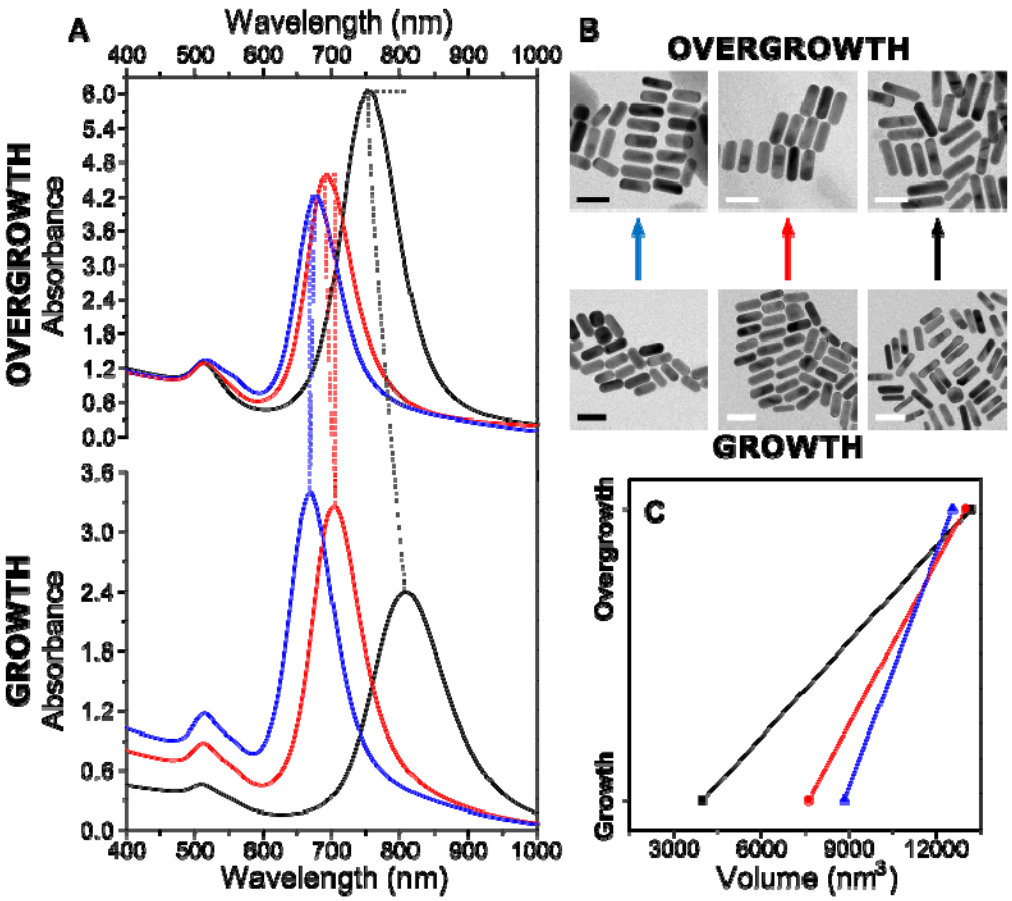

Figure 3. UV-visible spectra (**A**), TEM images (**B**) and average volume/NR (**C**) registered after the addition of AA to three NRs solutions prepared with different pre-reduction times as defined by Abs_{396nm}: 0.88 (black), 0.44 (red), 0.23 (blue). Note that the absorbance at 400 nm and the average volume/NR match upon overgrowth, whereas the longitudinal LSPR bands do not overlap. Scale bars: 50 nm. UV-vis spectra were multiplied by the corresponding dilution factor).

It is also important to study the effect of 5-BrSA concentration. The reduction rate of Au(III) to Au(I) decreases for lower 5-BrSA concentration, but tracking the reduction through the absorbance at 396 nm allowed us to initiate the reduction of Au(I) to Au(0) –upon ascorbic acid addition– at the same starting conditions, i.e. the same amount of consumed electrons. This

means that the pre-reduction time can be considered constant, as well as the concentration of AA. We carried out three experiments in which the concentrations of 5-BrSA were: 4.1, 2.3 and 0.9 mM. Whereas the absorbance at 400 nm reached the same value, the final position of the longitudinal plasmon band is shorter for lower concentrations of 5-BrSA (Figure 4A). The NR dimensions confirmed the trend observed in the optical properties, indicating that smaller amounts of 5-BrSA lead to NRs with a lower AR (Supporting Information, Table S1). Once again, the reduction ends before the blue shift does, confirming the coexistence of isotropic growth and reshaping. TEM analysis upon thiol addition (Figure 4B) confirmed that the initial well-defined nanorods (a1, a2, a3) progressively grow (volume increase) until the end of the reduction step (b1, b2, b3), after which the average volume per particle remains constant (c1, c2, c3; and Figure S7, Supporting Information). Importantly, we observed that 5-BrSA also affects the reduction rate of Au(I) to Au(0). This effect cannot be explained with a change in the pH of the solution, since the difference is always lower than 0.35 pH units. Thus, besides changing the number of electrons provided to the system, larger amounts of 5-BrSA were also found to lead to a decrease in the rate of gold reduction (Figure 4A). This suggests that 5-BrSA actively contributes to the growth, thereby revealing its role as co-factor. In fact, Murray and co-workers[9] attributed the role of salicylic acid to stabilization of the CTAB bilayer by the negatively charged aromatic additives. Molecular interactions between small additives and surfactant molecules facilitate the intercalation of such additives in the surfactant bilayer, which in turn improves its compactness. In such a scenario, the decrease of available catalytic surface slows down the overall reduction rate. We propose that tightly organized molecules on the lateral NR faces prevent mass transport (of metal salt) through the bilayer, thereby facilitating preferential metal reduction on the tips, and promoting anisotropic growth. This argument may also explain how

oleic acid can help creating more robust systems that can stand different synthetic conditions, thereby leading to different sizes, ARs (or shapes) and crystallographic habits of the nanoparticles.[8]

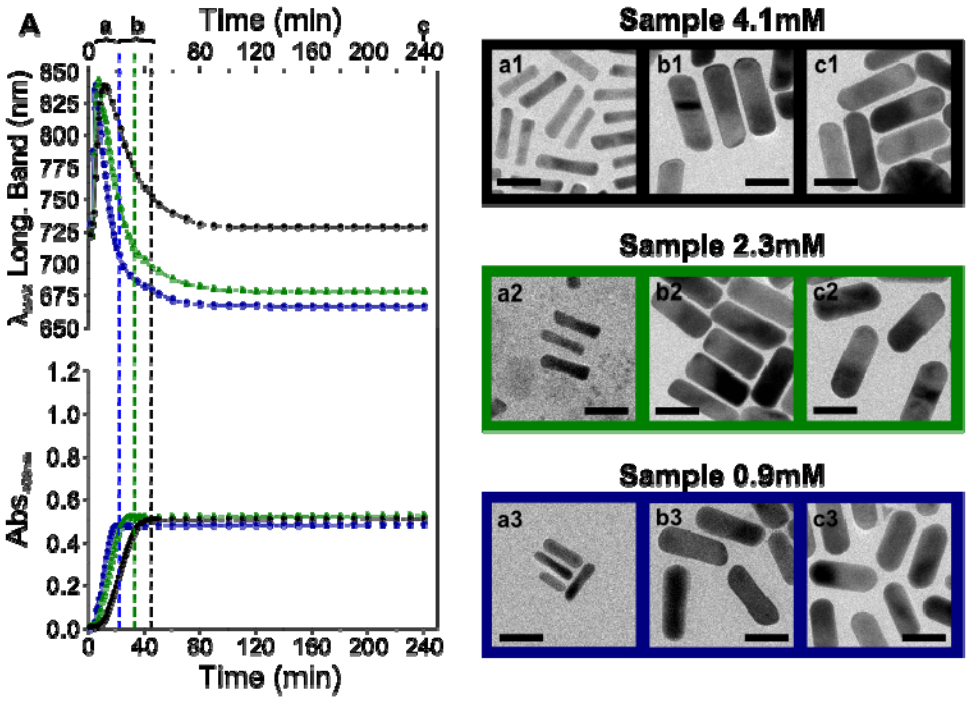

Figure 4. Effect of 5-BrSA concentration. **A:** Time traces of the longitudinal LSPR and absorbance at 400 nm during the growth of Au NRs using different 5-BrSA concentrations. [5-BrSA] = 4.1 mM (1, black), 2.3 mM (2, green) and 0.9 mM (3, blue). The three vertical dashed lines indicate the times at which no further gold reduction is observed for each sample, whereas a, b and c correspond to the times at which the growth was arrested by thiol addition. **B:** Representative TEM images for the three samples, collected after addition of dodecanethiol. The labels identify the three times at which the synthesis was stopped (a, b, c) and the imaged sample, 4.1 mM (1), 2.3 mM (2), 0.9 mM (3). Scale bars: 30 nm.

Overgrowth. We identify as a major advantage of using 5-BrSA its inability to reduce Au(I) into Au(0), even in the presence of gold seeds. Therefore, solutions can be prepared containing Au(I) (complexed to CTAB) and chemically stable Au(0) seeds, thereby avoiding the problem of eventual comproportionation reactions, which lead to the dissolution of metallic gold particles when mixed with Au(III)-CTAB.[23,27,28] In this way, experimental protocols for the synthesis of core-shell nanoparticles can be facilitated. We demonstrate this by using preformed NRs as seeds for additional growth (Overgrowth). The experimental procedure (see Scheme S2, Supporting Information) comprises the dispersion of AuNRs in an overgrowth solution prepared by complete pre-reduction of Au(III) to Au(I) with 5-BrSA, followed by addition of ascorbic acid. Note that the dispersion containing AuNRs and Au(I) can be stored over extended periods of time without any sign of NR oxidation. We exploited this possibility to further control the LSPR shift during overgrowth. In particular, we compared the influence of Ag^+ ions on the overgrowth process (Figure S8, Supporting Information): three solutions of NRs with different ARs were centrifuged and redispersed in two different solutions of Au(I), one of which contained Ag^+ (0.096mM); the amount of gold was the same as that used for initial NR growth (25 μmol of $HAuCl_4$), i.e. the concentration needed to reach an optical density of 1.2 at 400 nm. We observed in both cases a blueshift of the longitudinal LSPR, though not in the same extent, indicating that the AR of the resulting NRs was higher in the presence of Ag^+, which was confirmed by TEM analysis, showing in this case longer and thinner NRs (Figure S8 and Table S2, Supporting Information). This methodology offers the possibility of being implemented in multiple cycles, thereby opening new possibilities for tuning the dimensions of the NRs.

Multicycle Ag-free Overgrowth. The result of several growth cycles on preformed NRs is depicted in Figure 5. It can be clearly observed that after four overgrowth cycles performed under Ag-free conditions the NRs became essentially isotropic (Figure 5C). The spectral evolution (Figure 5A) agrees with that previously reported for a rod-to-octahedron transition,[29,30] which was again confirmed by TEM, showing a gradual increase in particle size (for details concerning dimensions and additional images see Figures S8-S10 and Table S3, Supporting Information). It is important to note that the absorbance at 400 nm increases by 1.2 after each overgrowth cycle (to 2.4, 3.6, 4.8 6.0), evidencing quantitative reduction of all additional gold ions in the growth solution.

Multicycle Ag-assisted Overgrowth. When overgrowth was performed under standard Ag-assisted conditions, the AR decreased from 3.0 to 2.4 after two cycles, but it then remained constant around this value (Figure 5C). Optical analysis showed that the longitudinal LSPR remained around 700 nm despite of the increase in NR volume (Figure 5B, Figures S9-S11 and Table S3, Supporting Information). An additional observation concerns the ratio between longitudinal and transverse plasmon bands, since the band centered at 530 nm shows an important absorbance increase. This can be rationalized considering two factors: first of all the larger diameter of the NRs has been demonstrated by calculation to increase the transversal contribution to the optical profile.[31] Additionally, the samples were not purified before the overgrowth step, so that spherical impurities were overgrown along with the NRs, thereby increasing their contribution to the absorbance of the low wavelength band. The stabilization of the AR points toward preferential adsorption of Ag^+ ions on the side facets of the growing nanoparticles, thereby enhancing the stability of the rod-like morphology. This can explain why the yield in nanorod formation increases when Ag^+ is added to the growth solution, and why

under typical synthetic conditions it is difficult to obtain NRs with high AR values, as compared to Ag-free synthesis,[20] but additional experimental evidences may be needed to elucidate this point. The protocol we propose here sets no limitations on the composition of the overgrowth solution, and thus can in principle be applied to nanoparticles with different shapes or compositions, to ultimately tune their optical properties, size and morphology or to easily access bimetallic systems.

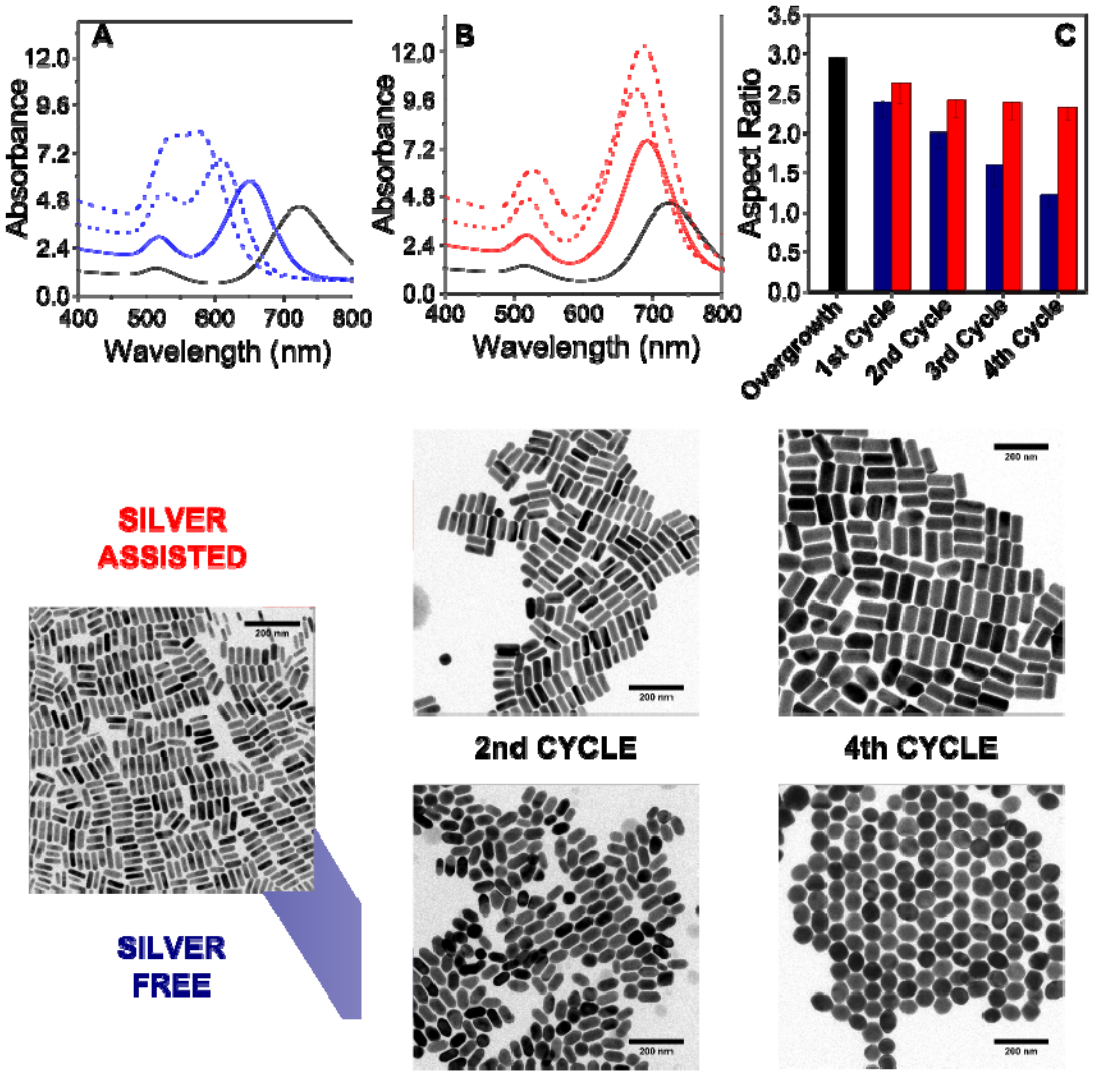

Figure 5. Upper Panel: Visible-NIR spectra after each overgrowth step. **A:** Silver-free system; **B:** Silver-assisted system. The black spectra correspond to the common starting point for the overgrowth reactions (UV-vis spectra were multiplied by the corresponding dilution factor). **C:** Evolution of the aspect ratio for each overgrowth cycle in both silver-free (blue) and silver-assisted (red) systems. **Lower Panel:** TEM images showing the shape evolution from the initial sample (central-left image) after two and four cycles for silver-free (blue line) and the silver-assisted (red line) conditions. Scale bars: 200 nm.

CONCLUSIONS

We have systematically studied the effect of salicylic acid on the synthesis of gold nanorods, both as stabilizing co-factor and as pre-reducing agent. We showed that this two-reducing-agents system offers new possibilities toward tailoring the morphology and the optical properties of Au NRs. We also showed that there is a direct relationship between the reduction yield and the total amount of electrons supplied to the system, thus demonstrating the possibility of quantitative gold reduction in Ag-mediated NR synthesis. Our observations indicate that 5-BrSA influences the growth reaction both thermodynamically and kinetically, inhibiting the isotropic growth that contributes to the typically observed blueshift in Au NRs synthesis. These results underline that the growth rate is an extremely important parameter in determining the morphology of the synthesized particles, in line with what has been recently proposed in the literature.[32–34] When reduction is not completed during synthesis, the system can be pushed into complete reduction through the addition of AA, without losing the possibility to tune the AR of the NRs. Apart from the new mechanistic insights of these results, the reducing properties of 5-BrSA can be exploited

to stabilize Au nanorods in Au(I) solution, thereby facilitating overgrowth. We demonstrated that overgrowth can be carried out in the presence of Ag^+ ions, thereby stabilizing the anisotropy, i.e. avoiding a rod-to-octahedron transition, as registered in Ag-free overgrowth. This suggests the possibility of tailoring the dimensions and optical properties of gold NRs by selecting the appropriate conditions for overgrowth.

METHODS

Materials. Hexadecyltrimethylammonium bromide (CTAB, ≥96%), 5-bromosalicylic acid (technical grade, 90%), hydrogen tetrachloroaurate trihydrate ($HAuCl_4 \cdot H_2O$, ≥99.9%), silver nitrate ($AgNO_3$, ≥99.0%), L-ascorbic acid (≥99%), dodecanethiol (≥98%) and sodium borohydride ($NaBH_4$, 99%) were purchased from Aldrich. All the chemicals were used as received. Milli-Q water (resistivity 18.2MΩ·cm at 25 ºC) was used in all experiments. All glassware was washed with aqua regia, rinsed with water, sonicated three-fold for 3 min with Milli-Q water and dried before use.

Synthesis of Au NRs. The seeds were prepared by the standard CTAB/$NaBH_4$ procedure: 25μL of a 0.05 M $HAuCl_4$ solution was added to 4.7mL of 0.1M CTAB solution; 300 μL of a freshly prepared 0.01M $NaBH_4$ solution was then injected under vigorous stirring. Excess borohydride was consumed by keeping the seed solution for 30 min at room temperature prior to use. Gold nanorods were prepared, with some modifications, as previously described by Murray and co-workers.[9] In a typical synthesis of 50 mL NRs solution, 50 mg of 5-Br salicylic acid was added to 25 mL of 0.1M CTAB. After complete dissolution, 480 μL of 0.01M $AgNO_3$ was added. The

solution was left under mild stirring for 15 min at room temperature, then 25 mL of 0.001M $HAuCl_4$ solution was added to the mixture, starting the pre-reduction step. At the selected pre-reduction time, 130 μL of 0.1M AA solution was added under vigorous stirring, followed by 80 μL of seed solution. After 30s the stirring was stopped and the mixture was left undisturbed at room temperature for at least 4 hours. All the obtained nanorod solutions were used for the following steps without further purification.

Growth Arrest by Dodecanethiol Injection. NR growth was monitored by UV-visible spectroscopy. When the selected absorbance was reached, the growth was arrested by passivation of the NRs surface by direct injection of excess dodecanethiol to the cuvette. For 3 mL NRs solution, 100 μL of a 1M dodecanethiol in acetone solution was used.

Reduction of Unreacted Au(I). The fraction of unreacted Au(I) in solution was calculated by assuming 1.2 as the absorbance at 400 nm corresponding to complete reduction of the gold precursor into Au(0). The amount of 0.01 M AA solution required for the reduction (with 10% excess) was added under vigorous stirring using a syringe pump (model: WPI SP210IWZ); the average injection rate used was around 100 μL/h. This value can change significantly according to the volume, so that a total injection time around 6 hours was maintained. The overgrown samples were centrifuged (7000 rpm, 25 min, 29 ºC) and redispersed in an equal volume of 0.05M CTAB.

Overgrowth Reaction. 10 mL of a solution of CTAB (0.05 M), 5-Br salicylic acid (3.8 mM), $HAuCl_4$ (0.5 mM) and $AgNO_3$ (when present, 0.096 mM) was left undisturbed at room temperature until the reduction of the gold precursor to Au(I) was completed and the solution appeared transparent. This solution was then used to redisperse 10 mL of NRs after two

centrifugation steps (7000 rpm, 25 min, 29 ºC). The obtained mixture was stable at room temperature. Ascorbic acid (15% excess) was added under vigorous stirring using a syringe pump; the average injection rate was around 100 μL/h of 0.01M AA, but this value can significantly vary according to the volume, so that a total injection time around 6 hours was maintained. The samples were finally centrifuged (7000 rpm, 25 min, 29 ºC) and stabilized in 10 mL 0.1M CTAB.

Multicycle Overgrowth Reaction. This process comprises a simple repetition of the previous overgrowth process. The samples (50 mL) were centrifuged twice and redispersed in 2x25mL of a CTAB/5-Br salicylic acid/Au(I) solution (one with and one without Ag^{+}), to which ascorbic acid was added with a syringe pump under vigorous stirring. After each cycle 5 mL of solution was separated for characterization. As the particle size increased, centrifugation was carried out at a lower speed, and the excess of ascorbic acid was increased to ensure complete reduction: 1stCycle (15% excess, 5500 rpm, 20 min, 29 ºC), 2ndCycle (20% excess, 5000 rpm, 20 min, 29 ºC), 3rdCycle (25% excess, 4500 rpm, 15 min, 29 ºC), 4thCycle (30% excess, 4000 rpm, 15 min, 29 ºC).

Spectroscopic and Structural Characterization. Transmission electron microscopy (TEM) images were collected with a JEOL2010F FE-TEM instrument operating at 200kV with carbon-coated 400 square mesh copper grids; all the samples were centrifuged twice before blotting on the grid. Optical extinction spectra were recorded using an Agilent 8453 UV-vis diode-array spectrophotometer. All the presented UV-vis spectra were multiplied by the respective dilution factors to facilitate comparison of the data.

ASSOCIATED CONTENT

Supporting Information Available: Additional TEM images and UV-vis-NIR spectra, analysis of NPs dimensions and schematic graphic descriptions of the growth and overgrowth procedures. This information is available free of charge via the Internet at http://pubs.acs.org/.

ACKNOWLEDGEMENT. Funding is acknowledged from the European Research Council (PLASMAQUO, 267867). M.G. acknowledges the receipt of a fellowship from IKERBASQUE, the Basque Foundation for Science.

References

(1) DuChene, J. S.; Niu, W.; Abendroth, J. M.; Sun, Q.; Zhao, W.; Huo, F.; Wei, W. D. *Chem. Mater.* **2013**, *25*, 1392–1399.

(2) Gómez-Graña, S.; Goris, B.; Altantzis, T.; Fernández-López, C.; Carbo-Argibay, E.; Martínez, A. G.; Almora-Barrios, N.; Lopez, N.; Pastoriza-Santos, I.; Perez-Juste, J.; Bals, S.; Van Tendeloo, G.; Liz-Marzán, L. M. *J. Phys. Chem. Lett.* **2013**, *4*, 2209–2216.

(3) Nikoobakht, B.; El-Sayed, M. A. *Chem. Mater.* **2003**, *15*, 1957–1962.

(4) Grzelczak, M.; Pérez-Juste, J.; Mulvaney, P.; Liz-Marzán, L. M. *Chem. Soc. Rev.* **2008**, *37*, 1783–1791.

(5) Pérez-Juste, J.; Pastoriza-Santos, I.; Liz-Marzán, L. M.; Mulvaney, P. *Coord. Chem. Rev.* **2005**, *249*, 1870–1901.

(6) Hubert, F.; Testard, F.; Spalla, O. *Langmuir* **2008**, *24*, 9219–9222.

(7) Liu, M.; Guyot-Sionnest, P. *J. Phys. Chem. B* **2005**, *109*, 22192–22200.

(8) Ye, X.; Zheng, C.; Chen, J.; Gao, Y.; Murray, C. B. *Nano Lett.* **2013**, *13*, 765–771.

(9) Ye, X.; Jin, L.; Caglayan, H.; Chen, J.; Xing, G.; Zheng, C.; Doan-Nguyen, V.; Kang, Y.; Engheta, N.; Kagan, C. R.; Murray, C. B. *ACS Nano* **2012**, *6*, 2804–2817.

(10) Okamoto, S.; Hachisu, S. *J. Colloid Interface Sci.* **1977**, *62*, 172–181.

(11) Malikova, N.; Pastoriza-Santos, I.; Schierhorn, M.; Kotov, N. A.; Liz-Marzán, L. M. *Langmuir* **2002**, *18*, 3694–3697.

(12) Luo, Y. *Mater. Lett.* **2007**, *61*, 1346–1349.

(13) Yang, J. A.; Lohse, S. E.; Boulos, S. P.; Murphy, C. J. *J. Cluster Sci.* **2012**, *23*, 799–809.

(14) Park, K.; Drummy, L. F.; Wadams, R. C.; Koerner, H.; Nepal, D.; Fabris, L.; Vaia, R. A. *Chem. Mater.* **2013**, *25*, 555–563.

(15) Edgar, J. A.; McDonagh, A. M.; Cortie, M. B. *ACS Nano* **2012**, *6*, 1116–1125.

(16) Vigderman, L.; Zubarev, E. R. *Chem. Mater.* **2013**, *25*, 1450–1457.

(17) Grochola, G.; Snook, I. K.; Russo, S. P. *J. Chem. Phys.* **2007**, *127*, 194707–194719.

(18) Maltzahn, G. von; Park, J.-H.; Agrawal, A.; Bandaru, N. K.; Das, S. K.; Sailor, M. J.; Bhatia, S. N. *Cancer Res.* **2009**, *69*, 3892–3900.

(19) Orendorff, C. J.; Murphy, C. J. *J. Phys. Chem. B* **2006**, *110*, 3990–3994.

(20) Lohse, S. E.; Murphy, C. J. *Chem. Mater.* **2013**, *25*, 1250–1261.

(21) Johnson, C. J.; Dujardin, E.; Davis, S. A.; Murphy, C. J.; Mann, S. *J. Mater. Chem.* **2002**, *12*, 1765–1770.

(22) Pérez-Juste, J.; Liz-Marzán, L. M.; Carnie, S.; Chan, D. Y. C.; Mulvaney, P. *Adv. Funct. Mater.* **2004**, *14*, 571–579.

(23) Rodríguez-Fernández, J.; Pérez-Juste, J.; Mulvaney, P.; Liz-Marzán, L. M. *J. Phys. Chem. B* **2005**, *109*, 14257–14261.

(24) Yang, Y.; Wang, W.; Li, X.; Chen, W.; Fan, N.; Zou, C.; Chen, X.; Xu, X.; Zhang, L.; Huang, S. *Chem. Mater.* **2013**, *25*, 34–41.

(25) Sau, T. K.; Murphy, C. J. *Langmuir* **2004**, *20*, 6414–6420.

(26) Miranda, O. R.; Dollahon, N. R.; Ahmadi, T. S. *Cryst. Growth Des.* **2006**, *6*, 2747–2753.

(27) Khanal, B. P.; Zubarev, E. R. *J. Am. Chem. Soc.* **2008**, *130*, 12634–12635.

(28) Gole, A.; Murphy, C. J. *Chem. Mater.* **2004**, *16*, 3633–3640.

(29) Carbó-Argibay, E.; Rodríguez-González, B.; Pacifico, J.; Pastoriza-Santos, I.; Pérez-Juste, J.; Liz-Marzán, L. M. *Angew. Chem., Int. Ed.* **2007**, *46*, 8983–8987.

(30) Myroshnychenko, V.; Carbó-Argibay, E.; Pastoriza-Santos, I.; Pérez-Juste, J.; Liz-Marzán, L. M.; García de Abajo, F. J. *Adv. Mater.* **2008**, *20*, 4288–4293.

(31) Lee, K.-S.; El-Sayed, M. A. *J. Phys. Chem. B* **2005**, *109*, 20331–20338.

(32) Langille, M. R.; Personick, M. L.; Zhang, J.; Mirkin, C. A. *J. Am. Chem. Soc.* **2012**, *134*, 14542–14554.

(33) Gu, J.; Zhang, Y.-W.; Tao, F. (Feng) *Chem. Soc. Rev.***2012**, *41*, 8050–8065.

(34) Huang, M. H.; Chiu, C.-Y. *J. Mater. Chem. A* **2013**, *1*, 8081–8092.

TOC Graphic

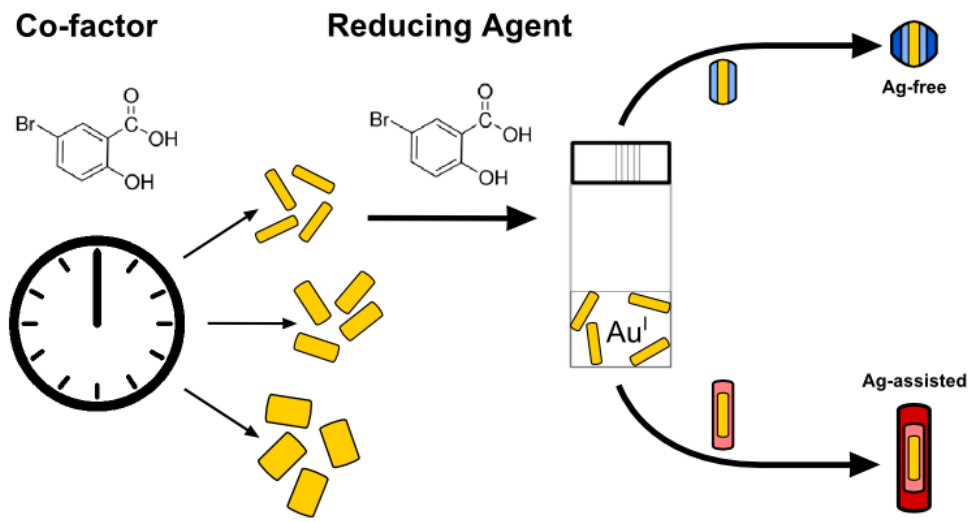
Co-factor
Reducing Agent
Br
O
C
OH
OH
Br
O
C
OH
OH
Au^{I}
Ag-free
Ag-assisted